Contribution from the Department of Chemistry,
Harvard University, Cambridge, Massachusetts 02138

Clusters Containing the $[ReFe_3(\mu_3\text{-}S)_4]$ Core: An Expansion of the Heterometal Cubane-Type Cluster Series MFe_3S_4

S. Ciurli, M. Carrié, and R. H. Holm*

Received February 15, 1990

From self-assembly systems containing $(Et_4N)[ReS_4]$, $FeCl_2$, and NaSEt in methanol, the three cluster complexes $(Et_4N)_3[Re_2Fe_6S_8(SEt)_9]$ (**7**), $(Et_4N)_2[Re_2Fe_7S_8(SEt)_{12}]$ (**8**), and $(Et_4N)_4[Re_2Fe_7S_8(SEt)_{12}]$ (**9**), containing $[ReFe_3(\mu_3\text{-}S)_4]$ cubane-type units, have been isolated in 66–84% yields as black, air-sensitive, crystalline solids. Compound **7** crystallizes in hexagonal space group $P6_3/m$ with a = 17.148 (5) Å, b = 17.148 (4) Å, c = 16.202 (2) Å, and Z = 2. Compound **8** was found in orthorhombic space group $Pcab$ with a = 12.316 (6) Å, b = 15.951 (5) Å, c = 38.44 (1) Å, and Z = 4. Compound **9** as its DMF monosolvate crystallizes in triclinic space group $P\bar{1}$ with a = 11.560 (3) Å, b = 11.691 (2) Å, c = 20.960 (8) Å, and Z = 1. The cluster structures consist of two terminal cubane-type $ReFe_3S_4(SEt)_3$ subclusters bridged through the Re atom by three μ_2-SEt sulfur atoms (**7**) or by a trigonal $(\mu_2\text{-}SEt)_3Fe(\mu_2\text{-}SEt)_3$ unit (**8**, **9**). In all cases the subclusters are related by an imposed center of symmetry. Structural data establish the presence of Fe(II) in the bridge units of **8** and **9**; consequently the subcluster core oxidation states are $2[ReFe_3S_4]^{4+}$ and $2[ReFe_3S_4]^{3+}$, respectively. Cluster **7** supports a five-member electron-transfer series and clusters **8** and **9** are part of a four-member series; in both, subcluster core oxidation states range from $[ReFe_3S_4]^{4+}$ (51 e) to $[ReFe_3S_4]^{2+}$ (53 e). Clusters **7** and **8** undergo stoichiometric terminal ligand substitution with 6 equiv of benzenethiol in acetonitrile solution to afford $[Re_2Fe_6S_8(SEt)_3(SPh)_6]^{3-}$ and $[Re_2Fe_7S_8(SEt)_6(SPh)_6]^{2-}$. These and other clusters can be identified by their characteristic isotropically shifted ^1H NMR spectra. Property comparisons are made with the previously reported Mo and W clusters $[M_2Fe_6S_8(SR)_9]^{3-}$ and $[M_2Fe_7S_8(SR)_{12}]^{3-,4-}$, which are congruent in structure with **7** and **8**/**9**, respectively. These new compounds extend the set of MFe_3S_4 cubane-type clusters to those with M = V, Mo, W, and Re, which include the isoelectronic subset $[VFe_3S_4]^{2+} = [MoFe_3S_4]^{3+} = [WFe_3S_4]^{3+} = [ReFe_3S_4]^{4+}$ (51 e). The clusters define a stability plateau associated with cores containing 50–53 e, with the 51-e species having special stability.

Introduction

An extensive set of heterometal cubane-type clusters containing the $MFe_3(\mu_3\text{-}S)_4$ cores with M = Mo and W[1-6] and V[5-9] has been synthesized. Molybdenum-containing clusters first were prepared in 1978–9 and were followed shortly by those containing tungsten.[1] The initial example of a VFe_3S_4 cluster was obtained in 1986.[7] Very recently, we have demonstrated the existence of the $ReFe_3S_4$ cluster in the double-cubane molecule $[Re_2Fe_7S_8(SEt)_{12}]^{2-}$.[10] Clusters incorporating these four heterometals are readily prepared by self-assembly from simple reactants.[1,8,10-13] Under the reaction conditions, which involve the appropriate tetrathiometalate $[MS_4]^{z-}$, an Fe(II,III) salt, and halide or thiolate, series 1 of isoelectronic (51 e) cores are formed.

$$[VFe_3S_4]^{2+} \quad [MoFe_3S_4]^{3+} \quad [WFe_3S_4]^{3+} \quad [ReFe_3S_4]^{4+} \qquad (1)$$

The reaction pathway by which a core is assembled is known only for the cluster $[VFe_3S_4Cl_3(DMF)_3]^{1-}$.[8] Redox reactions of clusters containing these cores permit access to other oxidation levels, with the result that a stability plateau at 50–53 e is apparent.

The potential for an extensive chemistry of $ReFe_3S_4$ clusters is suggested by analogy to the self-assembly of $MoFe_3S_4$ clusters and certain of their reactions, as summarized in Figure 1. The indicated assembly system affords as principal products three double-cubane clusters, $[Mo_2Fe_6S_8(SR)_9]^{3-}$ (**1**), $[Mo_2Fe_6S_9(SR)_8]^{3-}$ (**2**), and $[Mo_2Fe_7S_8(SR)_{12}]^{3-,4-}$ (**3**). Relative yields are dependent upon reaction stoichiometry and other factors,[11,12] with cluster salts being obtained in pure form by fractional recrystallization. The two clusters of structure **3** contain either Fe(II) or Fe(III) in the bridge. Other clusters are recoverable from **1** and **3**.[1] Thus, the reaction of **1** (R = Ph) with acenaphthylenide affords doubly reduced double cubane **4**.[14] Cleavage of **3** with catecholate or 1,2-bis(dimethylphosphino)ethane[4] affords the solvated single cubanes **5**, which react with various neutral and anionic ligands to give **6**.[2] In addition, there are doubly bridged double cubanes (not shown) which in solution dissociate to form,[1,2] or may be prepared from,[15] single cubane **5**. Structures **1**–**5** have also been demonstrated for WFe_3S_4 clusters. The chemistry of VFe_3S_4 clusters is quite different. The assembly system yields a single cubane directly.[7,8] While Fe sites have a strong affinity for both thiolate and chloride ligands, the vanadium site has little proclivity for either[6,8] and does not form the bridged structures in Figure 1.

We have begun an investigation of the syntheses, structures, and reactions of $ReFe_3S_4$ clusters, with the expectation that some of the structural patterns found with molybdenum- and tungsten-containing clusters will occur. We also anticipate that there will be meaningful differences in reactivity at the rhenium site, perhaps more noticeably with nitrogenous ligands. We report here our entry to $ReFe_3S_4$ clusters of two types in two oxidation levels by self-assembly, proof of cubane-type cluster structures by X-ray analysis, and several reactivity properties. Certain clusters derived from $[ReS_4]^-$, a starting material in our cluster assembly system, have been reported,[17-19] but these are not closely related to the clusters described here.

(1) Holm, R. H.; Simhon, E. D. In *Molybdenum Enzymes*; Spiro, T. G., Ed.; Wiley-Interscience: New York, 1985; Chapter 2. This paper contains a detailed summary of research on M = Mo and W clusters to 1984.
(2) Palermo, R. E.; Singh, R.; Bashkin, J. K.; Holm, R. H. *J. Am. Chem. Soc.* **1984**, *106*, 2600.
(3) Kovacs, J. A.; Bashkin, J. K.; Holm, R. H. *J. Am. Chem. Soc.* **1985**, *107*, 1784.
(4) Zhang, Y.-P.; Bashkin, J. K.; Holm, R. H. *Inorg. Chem.* **1987**, *26*, 694.
(5) Carney, M. J.; Kovacs, J. A.; Zhang, Y.-P.; Papaefthymiou, G. C.; Spartalian, K.; Frankel, R. B.; Holm, R. H. *Inorg. Chem.* **1987**, *26*, 719.
(6) Ciurli, S.; Holm, R. H. *Inorg. Chem.* **1989**, *28*, 1685.
(7) Kovacs, J. A.; Holm, R. H. *J. Am. Chem. Soc.* **1986**, *108*, 340.
(8) Kovacs, J. A.; Holm, R. H. *Inorg. Chem.* **1987**, *26*, 702.
(9) Kovacs, J. A.; Holm, R. H. *Inorg. Chem.* **1987**, *26*, 711.
(10) Ciurli, S.; Carney, M. J.; Holm, R. H.; Papaefthymiou, G. C. *Inorg. Chem.* **1989**, *28*, 2696.
(11) Wolff, T. E.; Berg, J. M.; Hodgson, K. O.; Frankel, R. B.; Holm, R. H. *J. Am. Chem. Soc.* **1979**, *101*, 4140.
(12) Wolff, T. E.; Power, P. P.; Frankel, R. B.; Holm, R. H. *J. Am. Chem. Soc.* **1980**, *102*, 4694.
(13) Christou, G.; Garner, C. D. *J. Chem. Soc., Dalton Trans.* **1980**, 2354.
(14) Christou, G.; Mascharak, P. K.; Armstrong, W. H.; Papaefthymiou, G. C.; Frankel, R. B.; Holm, R. H. *J. Am. Chem. Soc.* **1982**, *104*, 2820.
(15) Coucouvanis, D.; Challen, P. R.; Koo, S.-M.; Davis, W. M.; Butler, W.; Dunham, W. R. *Inorg. Chem.* **1989**, *28*, 4181.
(16) Do, Y.; Simhon, E. D.; Holm, R. H. *Inorg. Chem.* **1985**, *24*, 4635.
(17) Müller, A.; Krickemeyer, E.; Baumann, F.-M.; Jostes, R.; Bögge, H. *Chimia* **1986**, *40*, 310.
(18) Müller, A.; Krickemeyer, E.; Bögge, H. *Z. Anorg. Allg. Chem.* **1987**, *554*, 61.
(19) Müller, A.; Krickemeyer, E.; Bögge, H. *Angew. Chem., Int. Ed. Engl.* **1986**, *25*, 990.

0020-1669/90/1329-3493$02.50/0

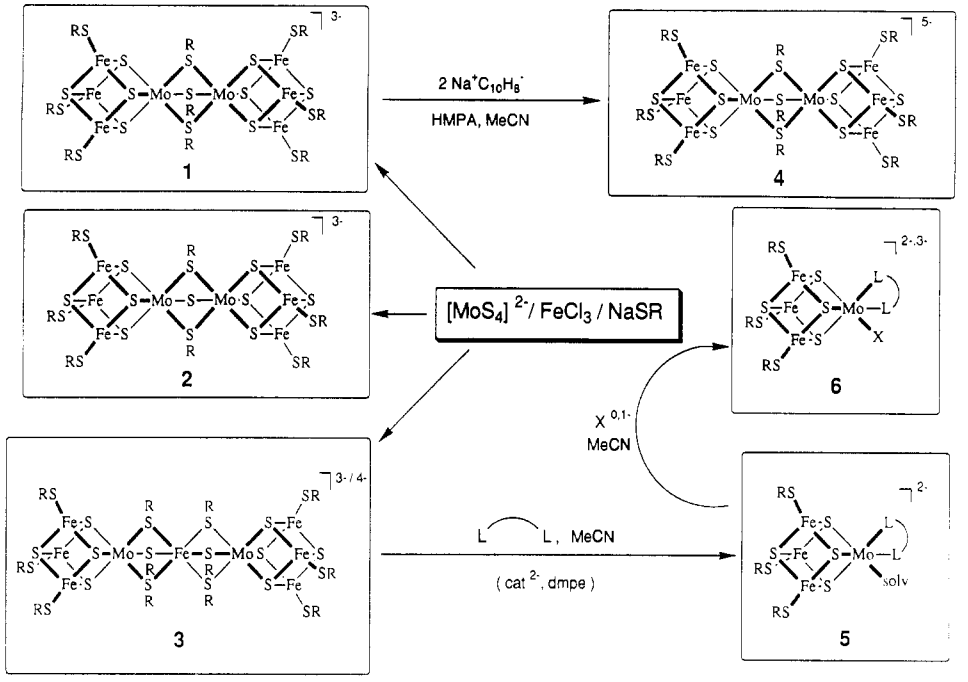

Figure 1. Schematic illustration of the synthesis of $[MoFe_3S_4]$ cubane-type clusters 1–3 by self-assembly methods and certain of their reactions including reduction of **1** to **4**, bridge cleavage of **3** to form single cubane **5**, and reactions of **5** at the Mo site to afford the substituted single cubanes **6**.

Experimental Section

Preparation of Compounds. All operations were carried out under a pure dinitrogen atmosphere; solvents were purified by standard procedures and degassed immediately before use. DMF (Burdick and Jackson, high purity, 0.03% H_2O) and deuterated solvents were dried over 3-Å molecular sieves. Steps of solvent removal and drying of solids were carried out in vacuo at room temperature. $(Et_4N)[ReS_4]$ was prepared according to a literature method.[18] $FeCl_2$ (Cerac, 99.99%) and all other reagents were used as received. ^1H NMR data are given for cluster anions (b = bridging, t = terminal); cation resonances are in their usual positions.

$(Et_4N)_3[Re_2Fe_6S_8(SEt)_9]$ (7). (a) By Self-Assembly. The brown solution prepared from $FeCl_2$ (2.85 g, 22.5 mmol) and NaSEt (5.70 g, 67.8 mmol) in 200 mL of ethanol was added to a purple slurry of $(Et_4N)[ReS_4]$ (2.85 g, 6.41 mmol) and Et_4NCl (0.5 g, 3.0 mmol) in 50 mL of ethanol. After the mixture was stirred for 24 h, a green-brown solution was obtained. This solution was refluxed for 24 h, giving a suspension of dark microcrystalline solid in a green solution. The solvent was removed and the residue suspended in acetonitrile. The mixture was stirred for 2 h and filtered to remove undissolved white solid. The residue obtained after removal of the filtrate solvent was suspended in 150 mL of ethanol, and 350 mL of ether was added with stirring. The suspension was allowed to stand at −20 °C overnight. The microcrystalline solid was collected, washed with ether, and dried to afford 3.85 g of green-black product, which was pure by ^1H NMR spectroscopy. A second crop (1.25 g, combined yield 84%) was isolated from analogous work-up of the mother liquor. An analytical sample was obtained by recrystallization from ethanol/ether. Anal. Calcd for $C_{42}H_{105}Fe_6N_3Re_2S_{17}$: C, 26.48; H, 5.56; Fe, 17.59; N, 2.21; Re, 19.55; S, 28.61. Found: C, 26.69; H, 5.29; Fe, 17.27; N, 2.01; Re, 18.81; S, 29.97. Absorption spectrum (DMF): λ_{max} (ϵ_M) 276 (62 700), 395 nm (42 000). ^1H NMR (300 K, CD_3CN, anion): δ 1.60 (b-CH_3), 9.70 (t-CH_3), 17.8 (b-CH_2), 61.5, 62.9 (t-CH_2).

(b) From (9). A green solution of $(Et_4N)_4[Re_2Fe_7S_8(SEt)_{12}]$ (**9**; vide infra) (0.30 g, 0.13 mmol) in 50 mL of ethanol was refluxed gently for 16 h. The green-brown solution obtained was filtered, and the volume was reduced to 10 mL. Ether (100 mL) was added, and the solution was allowed to stand at −20 °C overnight. The dark microcrystalline material was collected, washed with ether, and dried to yield 0.18 g (72%) of product pure by ^1H NMR spectroscopy.

$(Et_4N)_2[Re_2Fe_7S_8(SEt)_{12}]$ (8). (a) By Self-Assembly. A light brown slurry of $FeCl_2$ (1.70 g, 13.4 mmol), NaSEt (2.25 g, 26.7 mmol), and Et_4NCl (0.40 g, 2.41 mmol) in 200 mL of methanol was added to a purple slurry of $(Et_4N)[ReS_4]$ (1.00 g, 2.25 mmol) in 50 mL of methanol. After the mixture was stirred for 48 h, a slurry of dark brown microcrystalline solid in a green-brown solution was obtained. The solid was collected, washed with methanol, and extracted into 200 mL of acetonitrile. The red-brown mixture was stirred for 2 h and filtered, and the volume of the filtrate was reduced to 30 mL. Ether (200 mL) was added very slowly, with stirring. The dark brown microcrystalline solid that separated was collected, washed with ether, and dried to yield 1.50 g (66%) of product pure by ^1H NMR spectroscopy. An analytical sample was obtained as black crystals by recrystallization from acetonitrile/ether. Anal. Calcd for $C_{40}H_{100}Fe_7N_2Re_2S_{20}$: C, 23.90; H, 5.00; Fe, 19.41; N, 1.39; Re, 18.49; S, 31.83. Found: C, 24.50; H, 4.72; Fe, 19.51; N, 1.38; Re, 17.49; S, 32.25. Absorption spectrum (DMF): λ_{max} (ϵ_M) 290 (91 000), 392 nm (57 000). ^1H NMR (298 K, CD_3CN, anion): δ −25.0 (b-CH_3), 10.8 (t-CH_3), 77.2 (t-CH_2), 84 (b-CH_2, 332 K).

(b) From (9). A blue solution of $(Cp_2Fe)BF_4$ (0.12 g, 0.44 mmol) in 2 mL of acetonitrile was added dropwise to a stirred green solution of **9** (vide infra) (0.50 g, 0.22 mmol) in 20 mL of acetonitrile. The color changed to red-brown, and the resulting solution was stirred for 15 min. The solvent was removed, and the residue was washed with ether until the washings were colorless. The ^1H NMR spectrum of the residue was consistent with a complete and clean reaction. Recrystallization from acetonitrile/ether afforded 0.26 g (59%) of crystalline black product pure by ^1H NMR spectroscopy.

$(Et_4N)_4[Re_2Fe_7S_8(SEt)_{12}]$ (9). A light brown slurry of $FeCl_2$ (0.85 g, 6.71 mmol), NaSEt (1.40 g, 16.6 mmol), and Et_4NCl (0.28 g, 1.69 mmol) in 100 mL of methanol was added to a purple slurry of $(Et_4N)[ReS_4]$ (0.50 g, 1.12 mmol) in 20 mL of methanol. The green-brown solution obtained after stirring the mixture for 48 h was filtered, and the filtrate solvent was removed. The residue was extracted into 100 mL of acetonitrile. Some white solid was removed by filtration, the filtrate volume was reduced to 30 mL, and ether (150 mL) was added with stirring. The black microcrystalline solid, which formed when this solution was maintained at −20 °C for 2 h, was collected, washed with ether, and dried to afford 0.95 g (75%) of product pure by ^1H NMR spectroscopy. An analytical sample was prepared by recrystallization from acetonitrile/ether. Anal. Calcd for $C_{56}H_{140}Fe_7N_4Re_2S_{20}$: C, 29.58; H, 6.20; Fe, 17.19; N, 2.46; Re, 16.37; S, 28.18. Found: C, 29.56; H, 5.29; Fe, 17.13; N, 2.28; Re, 15.38; S, 27.90. Absorption spectrum (DMF): λ_{max} (ϵ_M) 276 (88 000), 384 nm (54 000). ^1H NMR (297 K, CD_3CN, anion): δ −24.3 (b-CH_3), 12.8 (t-CH_3), 72.3 (t-CH_2), 81 (b-CH_2, 318 K).

X-ray Structural Determinations. Crystals were mounted with Apiezon grease in glass capillaries under a dinitrogen atmosphere and the capillaries were flame-sealed. Data collections were performed by using either a Nicolet P3F or a R3m four-circle diffractometer equipped with a Mo X-ray source and a graphite monochromator. For each compound, the orientation matrix and unit cell parameters were determined by the least-squares fit of the angular coordinates of 25 machine-centered reflections having $19° \leq 2\theta \leq 25°$. On the basis of three standard reflections whose intensities were measured periodically, the crystals showed no signs of decay during the course of the data collections. Intensity data were corrected for Lorentz and polarization effects by using the program XTAPE of the SHELXTL structure determination program

Table I. Summary of Crystal and Data Collection Parameters

	$(Et_4N)_3[Re_2Fe_6S_8(SEt)_9]$	$(Et_4N)_2[Re_2Fe_7S_8(SEt)_{12}]$	$(Et_4N)_4[Re_2Fe_7S_8(SEt)_{12}]\cdot DMF$
formula	$C_{42}H_{105}Fe_6N_3Re_2S_{17}$	$C_{40}H_{100}Fe_7N_2Re_2S_{20}$	$C_{59}H_{147}Fe_7N_5ORe_2S_{20}$
fw	1904.64	2013.57	2347.17
a, Å	17.148 (5)	12.316 (6)	11.560 (3)
b, Å	17.148 (4)	15.951 (5)	11.691 (2)
c, Å	16.202 (2)	38.44 (1)	20.960 (8)
α, deg			74.24 (2)
β, deg			86.57 (2)
γ, deg			61.65 (1)
V, Å^3	4125 (1)	7551 (5)	2391 (1)
Z	2	4	1
space group	$P6_3/m$	$Pcab$	$P\bar{1}$
T, K	193	298	298
λ, Å	0.710 69	0.710 69	0.710 69
ρ_{calc} (ρ_{obs}), g/cm^3	1.53 (1.52[a])	1.77 (1.79[b])	1.63 (1.62[a])
μ, cm^{-1}	44.3	25.6	40.3
R, %	3.86	7.11	9.83
R_w, %	4.56	10.78	10.69

[a] Determined by flotation in dibromomethane/chloroform. [b] Determined by flotation in dibromomethane/carbon tetrachloride.

package (Nicolet XRD Corp., Madison, WI 53711). Empirical absorption corrections were performed with the program PSICOR. Crystal data are summarized in Table I. Atomic scattering factors were taken from a standard source.[20]

(a) $(Et_4N)_3[Re_2Fe_6S_8(SEt)_9]$. Dark green needles were grown by diffusing ether into an ethanolic solution at room temperature. The compound crystallizes in the hexagonal system, and the systematic absences $000l$ ($l \neq 2n$) are consistent with space groups $P6_3$, $P6_3/m$, and $P6_322$. Analysis of the E map of the intensity data suggested a centric space group, and subsequent refinement in $P6_3/m$ to low error indices confirmed this choice.

(b) $(Et_4N)_2[Re_2Fe_7S_8(SEt)_{12}]$. Thin black plates were grown by layering ether onto an acetonitrile solution at room temperature. The compound crystallizes in the orthorhombic system, and the systematic absences $0kl$ ($l \neq 2n$), $h0l$ ($h \neq 2n$), $hk0$ ($k \neq 2n$), $h00$ ($h \neq 2n$), $0k0$ ($k \neq 2n$), and $00l$ ($l \neq 2n$) are consistent only with space group $Pcab$ (No. 61) (an unconventional setting of $Pbca$).

(c) $(Et_4N)_4[Re_2Fe_7S_8(SEt)_{12}]\cdot DMF$. Thin black plates were grown by diffusing ether into a DMF solution at room temperature. The crystal belongs to the triclinic system, and E statistics indicated the centrosymmetric space group $P\bar{1}$. This choice was confirmed by successful solution and refinement of the structure. The possibility that this compound belongs to a higher symmetry space group was ruled out by examination of the metric symmetry of the reduced cell matrix using TRACER.

Structure Solution and Refinement. (a) $(Et_4N)_3[Re_2Fe_6S_8(SEt)_9]$. All heavy atoms were located by direct methods with MULTAN. All remaining non-hydrogen atoms were located in successive difference Fourier maps and were refined by using SHELXTL. The asymmetric unit consists of one-sixth of the anion and half of a cation. The methyl carbon atoms of both the terminal and bridging thiolate groups were found to be disordered. In the terminal thiolate, the carbon atom is disordered over the two positions C(122) and C(123) with occupancies of 0.4 and 0.6, respectively, while the bridging carbon atom is disordered over two mirror-related positions C(132). Because of disorder in the thiolates and in the cation, only the Re, Fe, and S positions were refined anisotropically. In the final least-squares cycles, hydrogen atoms were placed 0.96 Å from bonded, nondisordered carbon atoms with an isotropic temperature factor of 0.08 Å^2. After the last cycle of refinement, each parameter shifted by <1% of its esd and the highest residual peak was equivalent to about 1.5 e/Å^2.

(b) $(Et_4N)_2[Re_2Fe_7S_8(SEt)_{12}]$. The structure was solved by direct methods using MULTAN. The E map derived from the phase set with the highest combined figures of merit revealed the trial positions of all Re, Fe, and S atoms. Refinement of this model with CRYSTALS led to the location of all remaining non-hydrogen atoms. The asymmetric unit consists of half of the anion and one cation. The anion has a crystallographically imposed inversion center located at the bridging iron atom. Isotropic refinement of this model converged to $R = 12.2\%$. All Re, Fe, S, and N atoms were refined anisotropically, whereas the C atoms were refined isotropically because of extensive thermal motion. The positions of the hydrogen atoms were calculated by setting C–H distances and hydrogen isotropic temperature factors at 0.96 Å and 0.08 Å^2, respectively. One of the terminal thiolate methyl groups was found to be disordered over the two positions C(13) and C(4), having occupancies of 0.4 and 0.6, respectively. Hydrogen atoms were not placed on the disordered thiolate group. After the last cycle of refinement, each parameter shifted by <1% of its esd. The highest two residual peaks, equivalent to 1.8 and 1.5 e/Å^2, were located in the vicinity of the Re atom.

Table II. Atomic Coordinates (×10^4) for $(Et_4N)_3[Re_2Fe_6S_8(SEt)_9]$

atom	x/a	y/b	z/c
Re	6667	3333	1406 (1)
Fe	6980 (1)	4363 (1)	20 (1)
S(1)	5701 (1)	3754 (1)	773 (1)
S(2)	6667	3333	−1014 (2)
S(3)	6957 (2)	4480 (2)	2500
S(4)	7372 (2)	5679 (2)	−585 (2)
C(121)	7663 (13)	6450 (12)	244 (11)
C(122)	8570 (30)	6934 (30)	384 (29)
C(123)	7756 (33)	7375 (29)	−240 (31)
C(131)	8139 (8)	5376 (8)	2500
C(132)	8278 (12)	6141 (12)	2031 (10)
N	4738 (6)	4086 (6)	−2562 (39)
C(11)	4355 (6)	4336 (6)	−3241 (5)
C(21)	4672 (6)	4179 (6)	−4080 (5)
C(12)	4461 (8)	3094 (8)	−2533 (27)
C(22)	3460 (9)	2441 (10)	−2596 (18)
C(14)	5758 (9)	4628 (9)	−2542 (44)
C(24)	6189 (9)	5629 (9)	−2587 (17)

(c) $(Et_4N)_4[Re_2Fe_7S_8(SEt)_{12}]\cdot DMF$. A Patterson map led to a trial position for the Re atom. All remaining non-hydrogen atoms were located in successive difference Fourier maps and were refined by using SHELXTL. The asymmetric unit consists of half of the anion, two cations, and half of a DMF solvate molecule. While the Re–Fe–S core is well defined, the terminal thiolate ligands, the cations, and the solvate molecule display extensive disorder and thermal motion, which required the application of constraints on interatomic distances involving the light atoms. For this reason, only the Re, Fe, and S atoms were refined anisotropically and no attempt was made to add calculated hydrogen atom positions in the final cycles of refinement. After the last cycle of refinement, each parameter shifted by <10% of its esd and the highest residual peak, equivalent to about 2 e/Å^2, was located in the vicinity of the Re atom.

Final agreement factors are included in Table I. Positional parameters are listed in Tables II–IV.[21]

Other Physical Measurements. All measurements were performed under strictly anaerobic conditions. ^{1}H NMR spectra were recorded on a Bruker AM 500 spectrometer using Me_4Si as internal reference. Absorption spectra were recorded with a Cary 219 spectrophotometer. Cyclic voltammetry and differential pulse polarography measurements were performed at room temperature, with a scan rate of 50 and 5 mV/s, respectively, in acetonitrile solution by using standard PAR instrumentation, a Pt working electrode, a SCE reference electrode, and 0.1 M $(Bu_4N)[BF_4]$ as supporting electrolyte.

Results and Discussion

Cluster Synthesis by Self-Assembly. The $MoFe_3S_4$ double-cubane clusters **1–3** have been readily prepared in satisfactory

(20) Cromer, D. T.; Waber, J. T. *International Tables for X-Ray Crystallography*; Kynoch: Birmingham, England, 1974.

(21) See paragraph at end of paper regarding supplementary material.

Table III. Atomic Coordinates ($\times 10^4$) for $(Et_4N)_2[Re_2Fe_7S_8(SEt)_{12}]$

atom	x/a	y/b	z/c
Re(1)	5687 (1)	111.4 (6)	4137.6 (3)
Fe(1)	5220 (4)	-457 (3)	3490 (1)
Fe(2)	5779 (5)	1169 (3)	3597 (1)
Fe(3)	7278 (4)	-62 (3)	3658 (1)
Fe(4)	5000	0	5000
S(1)	7067 (7)	1057 (5)	4009 (2)
S(2)	6297 (8)	-1123 (4)	3873 (2)
S(3)	4258 (8)	523 (5)	3780 (2)
S(4)	6365 (9)	317 (6)	3158 (2)
S(5)	4223 (13)	-1301 (8)	3169 (3)
S(6)	5523 (10)	2450 (6)	3396 (2)
S(7)	8969 (8)	-411 (7)	3528 (3)
S(8)	4310 (8)	-725 (4)	4463 (2)
S(9)	5034 (7)	1166 (4)	4568 (2)
S(10)	6719 (7)	-312 (4)	4667 (2)
N(1)	12802 (26)	1588 (19)	2629 (8)
C(1)	3693 (59)	-1991 (43)	3480 (18)
C(2)	2766 (63)	-1698 (44)	3609 (18)
C(3)	9442 (66)	-858 (52)	3985 (21)
C(4)	9854 (112)	-676 (84)	4141 (34)
C(5)	4982 (46)	3035 (31)	3744 (14)
C(6)	5733 (59)	3255 (44)	4006 (18)
C(7)	4686 (30)	-1843 (22)	4471 (10)
C(8)	3801 (35)	-2341 (25)	4667 (10)
C(9)	3635 (31)	1493 (22)	4470 (9)
C(10)	3308 (34)	2205 (26)	4700 (10)
C(11)	7733 (32)	465 (25)	4777 (10)
C(12)	8435 (35)	166 (24)	5079 (11)
C(13)	10608 (122)	-854 (87)	3927 (38)
C(14)	13566 (40)	2346 (29)	2640 (12)
C(15)	13269 (45)	3042 (33)	2871 (14)
C(16)	13297 (44)	985 (34)	2340 (14)
C(17)	14220 (44)	553 (32)	2462 (14)
C(18)	12771 (36)	1218 (28)	2996 (10)
C(19)	11984 (40)	501 (30)	3009 (11)
C(20)	11698 (42)	1882 (32)	2505 (14)
C(21)	11677 (38)	2354 (28)	2162 (12)

yield in the self-assembly system of Figure 1. These syntheses were conducted in methanol or ethanol and employed mole ratios at or near those required for stoichiometric cluster formation.[11-13] Analogous tungsten clusters are obtained with use of $[WS_4]^{2-}$. Consequently, assembly systems containing $(Et_4N)[ReS_4]/FeCl_3/NaSEt$ in various mole ratios at and above 1:3:6 were investigated in methanol solvent. In these systems, the principal product was a polymeric green iron thiolate together with very low yields of one or more of the clusters **7–9**. Inasmuch as a likely initial product of the system is $[S_2ReS_2Fe(SEt)_2]^-$, we concluded that $[ReS_4]^-$ is too weakly nucleophilic to cleave the thiolate polymer in a process that also would involve reduction to Fe(II) by thiolate.[22]

Replacement of $FeCl_3$ with $FeCl_2$ affords the successful assembly systems in Figure 2. Reactions 2–4 represent stoichiometric formation of the three clusters $[Re_2Fe_6S_8(SEt)_9]^{3-}$ (**7**),

$$2[ReS_4]^- + 6FeCl_2 + 13EtS^- \rightarrow [Re_2Fe_6S_8(SEt)_9]^{3-} + 12Cl^- + 2EtSSEt \quad (2)$$

$$2[ReS_4]^- + 7FeCl_2 + 14EtS^- \rightarrow [Re_2Fe_7S_8(SEt)_{12}]^{2-} + 14Cl^- + EtSSEt \quad (3)$$

$$2[ReS_4]^- + 7FeCl_2 + 16EtS^- \rightarrow [Re_2Fe_7S_8(SEt)_{12}]^{4-} + 14Cl^- + 2EtSSEt \quad (4)$$

(22) In the assembly system of Figure 1, the first detectable reaction product is $[S_2MoS_2Fe(SR)_2]^{2-}$, examples of which have been characterized.[1] In earlier work, we had observed the weaker coordinating ability of $[ReS_4]^-$ in the form of the equilibrium $[ReS_4]^- + [Fe(SPh)_4]^{2-} = [S_2ReS_2Fe(SPh)_2]^- + 2PhS^-$ in acetonitrile.[16] The Re species are present in ca. 1:1 mole ratio. In contrast, the corresponding reaction with $[MoS_4]^{2-}$ is complete. The lesser binding ability of $[ReS_4]^-$ derives from its lower negative charge and the diminished nucleophilicity of the sulfur atoms owing to the higher metal oxidation state.

Table IV. Atomic Coordinates ($\times 10^4$) for $(Et_4N)_4[Re_2Fe_7S_8(SEt)_{12}]\cdot DMF$

atom	x/a	y/b	z/c
Re(1)	-10042 (1)	10629 (1)	13304 (1)
Fe(1)	-9934 (3)	9556 (3)	12270 (2)
Fe(2)	-11454 (4)	12257 (3)	12111 (2)
Fe(3)	-8817 (4)	11173 (4)	12172 (3)
Fe(4)	0	10000	15000
S(1)	-10238 (7)	12730 (6)	12683 (4)
S(2)	-8173 (6)	9121 (7)	12890 (5)
S(3)	-11737 (6)	10564 (6)	12789 (4)
S(4)	-10099 (9)	11266 (9)	11349 (5)
S(5)	-9809 (10)	7761 (9)	12031 (7)
S(6)	-13339 (10)	14085 (10)	11606 (7)
S(7)	-7152 (11)	11545 (13)	11759 (9)
S(8)	-9890 (8)	8665 (6)	14209 (4)
S(9)	-11625 (6)	11835 (5)	14059 (4)
S(10)	-8503 (6)	10475 (6)	14150 (4)
C(51)	-8316 (25)	6442 (22)	12225 (15)
C(52)	-8203 (25)	5233 (23)	12823 (15)
C(61)	-14981 (18)	14333 (24)	11374 (13)
C(62)	-14795 (25)	14432 (25)	10544 (13)
C(72)	-5864 (24)	11634 (23)	12644 (14)
C(71)	-6840 (24)	12815 (19)	11962 (14)
C(81)	-8076 (22)	7286 (21)	14237 (14)
C(82)	-8102 (31)	6040 (31)	14663 (25)
C(91)	-13103 (22)	11682 (22)	14047 (14)
C(92)	-14022 (27)	12584 (26)	14314 (19)
C(101)	-8735 (21)	12196 (21)	14034 (14)
C(102)	-7703 (24)	12002 (24)	14587 (16)
N(1)	-13714 (16)	16971 (16)	13180 (12)
C(11)	-14492 (20)	17494 (20)	13749 (12)
C(12)	-14279 (28)	17195 (28)	14449 (22)
C(21)	-14283 (26)	18080 (23)	12531 (12)
C(22)	-13256 (34)	17495 (33)	12039 (30)
C(31)	-12270 (15)	16570 (26)	13307 (17)
C(32)	-11182 (34)	15930 (33)	13792 (30)
C(41)	-13829 (26)	15746 (20)	13133 (18)
C(42)	-14697 (33)	15772 (33)	12397 (30)
N(1′)	-13786 (16)	18216 (16)	13389 (12)
C(21′)	-14253 (27)	18744 (27)	12678 (11)
C(22′)	-13353 (33)	17903 (33)	12534 (30)
C(31′)	-12353 (15)	17276 (22)	13460 (17)
C(32′)	-12281 (34)	15619 (33)	13426 (30)
C(41′)	-14047 (26)	19345 (21)	13669 (18)
C(42′)	-15221 (34)	20044 (33)	13619 (30)
N(2)	-12957 (15)	21014 (15)	9900 (10)
C(111)	-13820 (21)	21400 (24)	9356 (12)
C(112)	-13724 (29)	21767 (28)	8665 (21)
C(221)	-12253 (21)	19619 (14)	10109 (14)
C(222)	-13622 (29)	19658 (28)	9852 (21)
C(331)	-13678 (23)	21508 (23)	10410 (12)
C(332)	-13609 (29)	20844 (28)	11271 (21)
C(441)	-12096 (19)	21538 (22)	9725 (15)
C(442)	-12893 (28)	23189 (28)	9678 (21)
C′	905 (21)	4984 (27)	9275 (23)
N′	528 (30)	4661 (31)	9998 (25)
C″	-441 (33)	5796 (32)	10286 (27)
O	187 (20)	5140 (25)	8899 (22)
C	1764 (32)	4933 (32)	10312 (28)

$[Re_2Fe_7S_8(SEt)_{12}]^{2-}$ (**8**), and $[Re_2Fe_7S_8(SEt)_{12}]^{4-}$, (**9**), which were prepared by self-assembly. Initial attempts were based on the stoichiometries $(Et_4N)[ReS_4]:FeCl_2:NaSEt = 1:(3.0–3.5):(6.5–10.5)$ in methanol at room temperature. These ratios cover those in reactions 2–4 but afforded combinations of black insoluble material, low yields of clusters, and unreacted $[ReS_4]^-$. Thereafter, it was found that the outcome of the assembly reactions was sensitive to the temperature and reactant mole ratios, these being in excess of the stoichiometric values for good yields.

The $(Et_4N)[ReS_4]:FeCl_2:NaSEt = 1:3.5:10.5$ system in refluxing ethanol gave **7** in 84% yield (based on Re) with no detectable amount of cluster byproducts. The 1:6:13 system afforded only **8** and **9** by ^1H NMR spectroscopy. The two compounds are readily separated by fractional crystallization because the Et_4N^+ salt of **8** is insoluble in methanol whereas that of **9** is soluble. Thereafter, the compounds were prepared free from each other

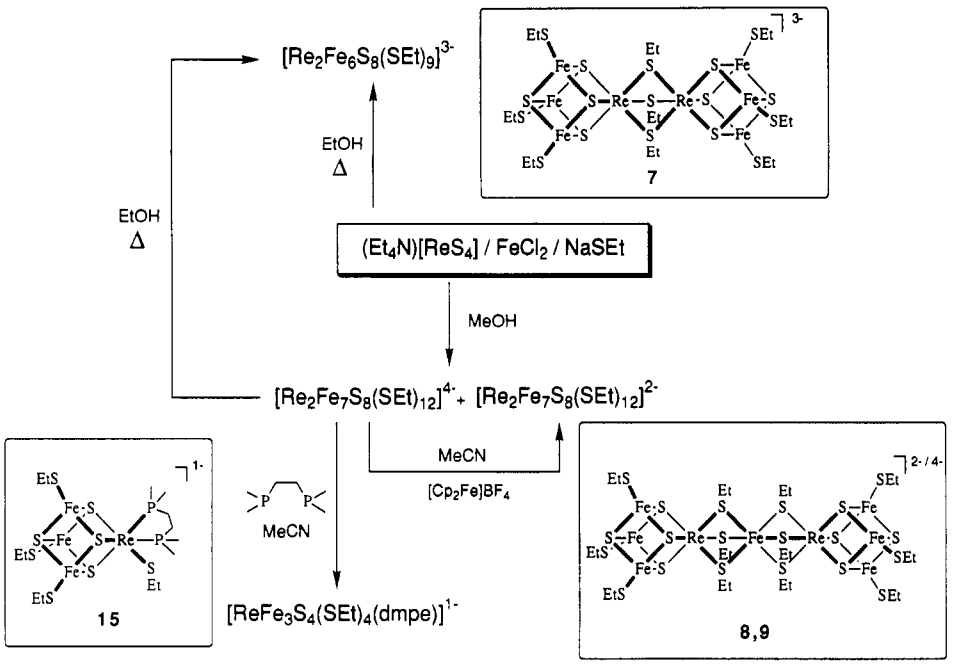

Figure 2. Scheme showing the reactions affording the $[ReFe_3S_4]$ cubane-type clusters **7–9** by self-assembly methods and the bridge cleavage of **8** to yield the single cubane **15**.

in the 1:6:12 (**8**) and 1:6:15 (**9**) systems in 66% and 75% yields, respectively. The implication from these ratios is that **9** is a reduction product of **8**, a matter confirmed by demonstration of the stoichiometric reaction (5) by ^1H NMR spectroscopy in

$$[Re_2Fe_7S_8(SEt)_{12}]^{2-} + 2EtS^- \rightarrow [Re_2Fe_7S_8(SEt)_{12}]^{4-} + EtSSEt \quad (5)$$

Me_2SO solution. By the same means, it was shown that **9** does not further react with a large excess of thiolate at room temperature. Refluxing a solution of **8** or **9** in ethanol produced **7**; in the case of **9**, the cluster was isolated in 72% yield. Evidently in the assembly systems, cluster **9** is formed first and is then degraded by refluxing into **7**, which has the same $[ReFe_3S_4]^{3+}$ core oxidation state. As shown in Figure 2, cluster **9** can be oxidized to **8**, which was isolated in 59% yield.

While we do not know the pathway of cluster assembly in any case, it is clear that the best results in the synthesis of clusters **7–9** are obtained in systems with iron and thiolate contents considerably above those required by stoichiometry. The stoichiometric reaction systems appear to be more complex than those empirically derived for synthetic purposes. Thus in reactions 2–4 there appear in the ^1H NMR spectra of the soluble products signals in the 60–70 ppm region that arise from two clusters not yet isolated or otherwise identified. Consequently, as many as five clusters are generated by the assembly system in Figure 2, depending on the mole ratio of reactants.

For reference in examining properties of clusters **7–9**, we first note the following isoelectronic relationships involving Mo, W, and Re species; electron counts refer to subclusters. Structurally characterized examples **10–14** and Mo or W clusters pertinent to the discussion that follows are indicated.

51 e:	$[Re_2Fe_7S_8(SEt)_{12}]^{2-}$ (**8**)	$[Mo_2Fe_6S_8(SR)_9]^{3-}$ (**1**) $[Mo_2Fe_7S_8(SR)_{12}]^{3-,4-}$ (**3**)
52 e:	$[Re_2Fe_6S_8(SEt)_9]^{3-}$ (**7**) $[Re_2Fe_7S_8(SEt)_{12}]^{4-}$ (**9**)	$[Mo_2Fe_6S_8(SR)_9]^{5-}$ (**4**)
	$[Mo_2Fe_6S_8(SEt)_9]^{3-}$ (**10**)[11] $[Mo_2Fe_6S_8(SPh)_9]^{5-}$ (**11**)[14] $[Mo_2Fe_7S_8(SEt)_{12}]^{3-}$ (**12**)[23]	$[Mo_2Fe_7S_8(SCH_2Ph)_{12}]^{4-}$ (**13**)[23] $[W_2Fe_7S_8(SCH_2Ph)_{12}]^{4-}$ (**14**)[23]

Cluster Structures. Clusters **7–9** were isolated as their Et_4N^+ salts, and their structures were crystallographically determined.

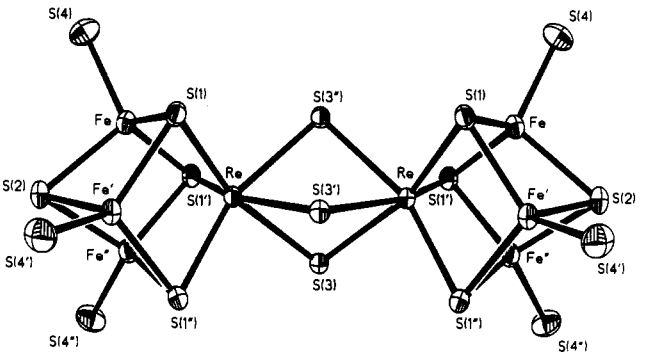

Figure 3. Structure of the cluster $[Re_2Fe_6S_8(SEt)_9]^{3-}$ (**7**), showing 50% probability ellipsoids and the atom-labeling scheme. Not included are the nine ethyl groups of the bridging and terminal thiolate ligands.

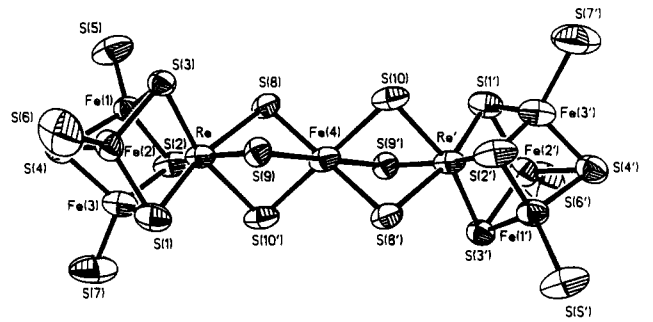

Figure 4. Structure of cluster the $[Re_2Fe_7S_8(SEt)_{12}]^{4-}$ (**9**), showing 50% probability ellipsoids and the atom-labeling scheme. Not included are the 12 ethyl groups of the bridging and terminal thiolate groups.

Crystal data are contained in Table I. The structure of **8** has been briefly reported earlier;[10] here additional structural details are provided. In all cases, the crystals contain discrete anions and cations. The cations exhibit extensive thermal motion and some disorder; in addition, some of the thiolate ligands also show disorder.

The structures of clusters **7** and **9** are shown in Figures 3 and 4, respectively. It is immediately seen that both are double-cubane clusters. In **7**, the anion contains two $ReFe_3S_4(SEt)_3$ subclusters bridged by three ethanethiolate groups through the Re atoms. In **8** and **9** the same cubane-type clusters are present, but they are

(23) Wolff, T. E.; Berg, J. M.; Power, P. P.; Hodgson, K. O.; Holm, R. H. *Inorg. Chem.* **1980**, *19*, 430.

Table V. Selected Interatomic Distances (Å) and Angles (deg) for Clusters **8** and **9**

	8	**9**		**8**	**9**
			Bridge Units		
Re···Re′	6.851 (2)	6.867 (2)	S(8)–Re–S(9)	79.0 (2)	79.7 (2)
Re···Fe(4)	3.425 (1)	3.433 (1)	S(8)–Re–S(10)	78.0 (3)	79.0 (3)
			S(9)–Re–S(10)	78.8 (2)	78.9 (2)
Re–S(8)	2.494 (8)	2.503 (7)			
Re–S(9)	2.492 (7)	2.493 (7)	Re–S(8)–Fe(4)	86.3 (2)	86.3 (2)
Re–S(10)	2.493 (8)	2.500 (9)	Re–S(9)–Fe(4)	86.8 (2)	86.2 (2)
			Re–S(10)–Fe(4)	86.1 (3)	85.7 (2)
Fe(4)–S(8)	2.514 (7)	2.519 (9)			
Fe(4)–S(9)	2.494 (7)	2.532 (6)	S(8)–Fe(4)–S(9)	78.6 (2)	78.7 (2)
Fe(4)–S(10)	2.523 (8)	2.550 (8)	S(8)–Fe(4)–S(10)	77.1 (3)	77.8 (3)
			S(9)–Fe(4)–S(10)	78.2 (2)	77.3 (2)
			S(8)–Fe(4)–S(9′)	101.4 (2)	101.3 (2)
			S(8)–Fe(4)–S(10′)	102.9 (3)	102.2 (3)
			S(9)–Fe(4)–S(10′)	101.8 (2)	102.7 (2)
			Clusters		
Re–S(1)	2.326 (8)	2.368 (7)	S(1)–Re–S(2)	102.6 (3)	101.4 (3)
Re–S(2)	2.340 (7)	2.343 (8)	S(1)–Re–S(3)	104.1 (3)	101.7 (3)
Re–S(3)	2.328 (9)	2.334 (9)	S(2)–Re–S(3)	102.9 (3)	101.8 (3)
Re···S(4)	3.870 (7)	3.97 (1)	S(1)–Re–S(9)	86.5 (3)	88.1 (2)
			S(1)–Re–S(10)	88.7 (3)	90.1 (3)
			S(2)–Re–S(8)	89.2 (3)	88.4 (3)
			S(2)–Re–S(10)	87.9 (3)	87.0 (3)
			S(3)–Re–S(8)	86.1 (3)	87.1 (3)
			S(3)–Re–S(9)	87.5 (3)	89.8 (3)
Re···Fe(1)	2.713 (4)	2.745 (5)	Re–Fe(3)–Fe(1)	60.3 (1)	60.0 (2)
Re···Fe(2)	2.680 (4)	2.752 (4)	Re–Fe(3)–Fe(2)	59.4 (1)	60.5 (1)
Re···Fe(3)	2.705 (4)	2.776 (6)			
			Re–S(1)–Fe(2)	71.7 (3)	73.3 (3)
Fe(1)···Fe(2)	2.715 (6)	2.723 (5)	Re–S(2)–Fe(1)	72.4 (3)	73.3 (2)
Fe(1)···Fe(3)	2.691 (7)	2.714 (8)	Re–S(2)–Fe(3)	72.4 (2)	74.1 (2)
Fe(2)···Fe(3)	2.705 (7)	2.685 (6)	Re–S(1)–Fe(3)	72.4 (3)	73.6 (2)
			Re–S(3)–Fe(1)	72.5 (3)	73.9 (2)
Fe(1)–S(2)	2.25 (1)	2.25 (1)	Re–S(3)–Fe(2)	71.6 (3)	73.5 (3)
Fe(1)–S(3)	2.257 (9)	2.233 (8)			
Fe(2)–S(1)	2.25 (1)	2.24 (1)	S(2)–Fe(1)–S(3)	108.2 (3)	108.1 (4)
Fe(2)–S(3)	2.25 (1)	2.264 (9)	S(1)–Fe(2)–S(3)	109.3 (3)	108.2 (3)
Fe(3)–S(1)	2.253 (8)	2.267 (9)	S(1)–Fe(3)–S(2)	108.4 (3)	107.2 (4)
Fe(3)–S(2)	2.238 (9)	2.261 (8)			
			S(2)–Fe(1)–S(4)	105.0 (4)	103.7 (4)
Fe(1)–S(4)	2.27 (1)	2.33 (1)	S(3)–Fe(1)–S(4)	103.2 (4)	103.7 (3)
Fe(2)–S(4)	2.283 (9)	2.30 (1)	S(1)–Fe(2)–S(4)	104.5 (4)	105.0 (4)
Fe(3)–S(4)	2.31 (1)	2.29 (1)	S(3)–Fe(2)–S(4)	102.8 (4)	103.5 (3)
			S(1)–Fe(3)–S(4)	103.6 (4)	104.5 (3)
Fe(1)–S(5)	2.20 (1)	2.22 (1)	S(2)–Fe(3)–S(4)	104.0 (4)	104.7 (4)
Fe(2)–S(6)	2.207 (9)	2.258 (9)			
Fe(3)–S(7)	2.21 (1)	2.24 (1)	S(4)–Fe(1)–S(5)	111.5 (5)	114.4 (5)
			S(4)–Fe(2)–S(6)	109.8 (4)	111.2 (5)
			S(4)–Fe(3)–S(7)	109.7 (4)	111.3 (6)
Fe(1)–Re–Fe(2)	60.5 (1)	59.4 (1)			
Fe(1)–Re–Fe(3)	59.6 (1)	58.9 (2)	Fe(2)–S(1)–Fe(3)	73.9 (3)	73.2 (3)
Fe(2)–Re–Fe(3)	60.3 (1)	58.1 (1)	Fe(1)–S(2)–Fe(3)	73.7 (3)	73.9 (3)
			Fe(1)–S(3)–Fe(2)	74.0 (3)	74.6 (2)
Re–Fe(1)–Fe(2)	59.2 (1)	60.4 (1)	Fe(1)–S(4)–Fe(2)	73.3 (3)	72.1 (3)
Re–Fe(1)–Fe(3)	60.1 (1)	61.1 (2)	Fe(1)–S(4)–Fe(3)	72.1 (3)	72.0 (3)
Re–Fe(2)–Fe(1)	60.4 (1)	60.2 (1)	Fe(2)–S(4)–Fe(3)	72.2 (3)	71.6 (4)
Re–Fe(2)–Fe(3)	60.3 (1)	61.4 (1)			

bridged by a $(SEt)_3Fe(SEt)_3$ unit, in which the central Fe atom resides in a trigonally distorted octahedral coordination sphere. In all cases, the terminal subclusters are related to each other by a crystallographically imposed center of symmetry, which, in **8** and **9**, is constituted by the bridge Fe atom.

The structure of **7** is closely related to that of $[Mo_2Fe_6S_8(SEt)_9]^{3-}$[11] (**10**) and $[Mo_2Fe_6S_8(SPh)_9]^{5-}$[14] (**11**), while **8** and **9** are essentially congruent in structure with $[Mo_2Fe_7S_8(SEt)_{12}]^{3-}$[23] (**12**) and $[M_2Fe_7S_8(SCH_2Ph)_{12}]^{4-}$[23] (M = Mo (**13**); M = W (**14**). Because the structures of the $MoFe_3S_4$ clusters have been described at length earlier,[1,11,14,23] we restrict considerations here to those comparative dimensional features dependent upon the nature of the heterometal and the subcluster oxidation state. Selected interatomic distances and angles for the three $ReFe_3S_4$ clusters are set out in Tables V and VI; a full listing of these parameters is available.[21] A summary of selected structural comparisons is presented in Table VII.

The mean bridge Fe–S distances of 2.51 (1) and 2.53 (3) Å in **8** and **9**, respectively, are consistent with Fe(II). When taken together with the results for **13** and **14**, the mean Fe^{II}–S bond distances in four $Fe(SR)_6$ bridge units fall into the interval 2.51–2.54 Å. In comparison, the analogous mean distance in the Fe(III)–bridged cluster **12** is 2.309 (9) Å. These bridge distances are the single most important metric structural result, for they substantiate the foregoing classification of isoelectronic structures. Thus, in passing from **8** to **9**, it is the subclusters that are primarily reduced.

Several additional observations are consistent with subcluster reduction, although a proof of this situation purely on a structural basis is difficult owing to the relatively large esd values of certain

Table VI. Selected Interatomic Distances (Å) and Angles (deg) for Cluster **7**

Re···Re	3.543 (1)	S(1)–Re–S(3)	87.8 (1), 91.2 (1)
		S(3)–Re–S(3)	75.5 (1)
Re···Fe	2.739 (1)	S(1)–Re–S(1)	102.3 (1)
Fe···Fe	2.715 (1)	S(1)–Fe–S(1)	108.2 (1)
		S(1)–Fe–S(2)	103.9 (1), 103.9 (1)
		S(1)–Fe–S(4)	116.5 (1), 115.8 (1)
Re–S(1)	2.348 (2)	S(2)–Fe–S(4)	107.1 (1)
Re···S(2)	3.924 (3)	Re–S(1)–Fe	73.0 (1), 73.0 (1)
Re–S(3)	2.505 (2)	Fe–S(1)–Fe	74.0 (1)
Fe–S(1)	2.257 (2), 2.256 (2)	Fe–S(2)–Fe	72.5 (1)
Fe–S(2)	2.294 (2)	Re–S(3)–Re	90.0 (1)
Fe–S(4)	2.232 (3)		

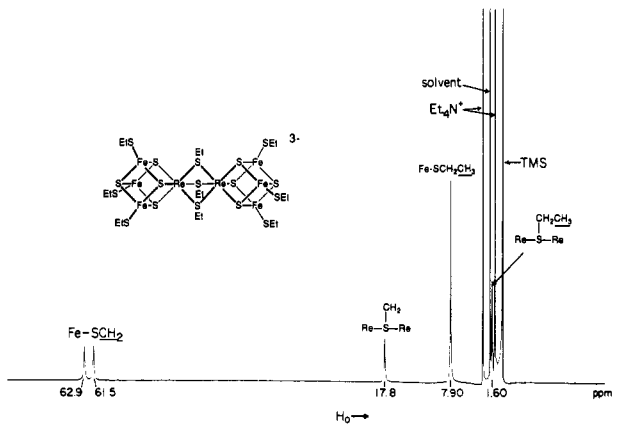

Figure 5. ^1H NMR spectrum of cluster **7** in MeCN-d_3 solution at 297 K. Signal assignments are indicated.

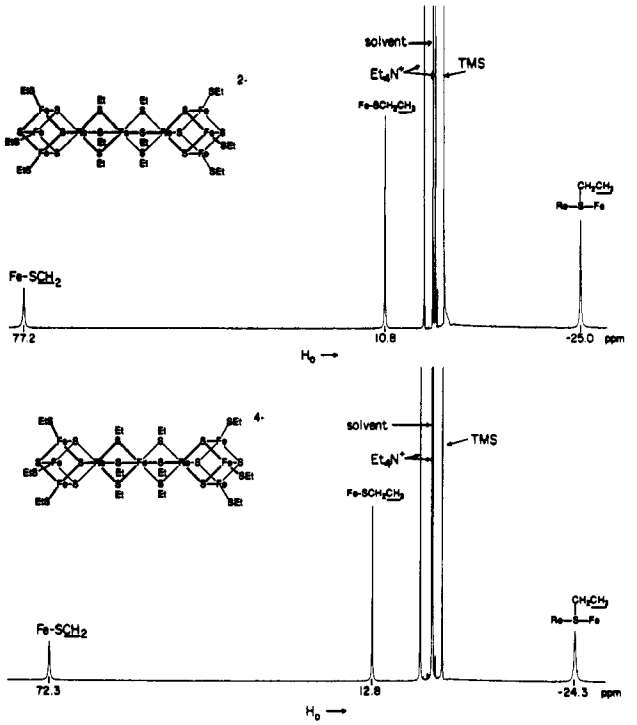

Figure 6. ^1H NMR spectra of cluster **8** (top) and cluster **9** (bottom) in MeCN-d_3 solution at 297 K. Signal assignments are indicated.

bond distances. (i) The subcluster dimensions of **7** and **9**, whose composition defines its 52 e oxidation level, are essentially identical. (ii) The mean terminal Fe–SR bond distance is about 0.03 Å longer in **9** than in **8**, consistent with increased Fe(II) core character in the former. In MFe_3S_4 and Fe_4S_4 clusters these distances *always* increase upon reduction, as found, e.g., in the ca. 0.05 Å difference between $[Mo_2Fe_6S_8(SPh)_9]^{3-}$ [24] and **11**.

Several other structural features are noted. (iii) The difference between bridge or cluster Re–S distances in **8** and **9** is essentially nil, whereas Shannon radii[25] predict a 0.03–0.05 Å difference if the localized, six-coordinate oxidation states Re(IV,V,VI) are involved. (iv) In the 51 e series **8** and **12–14**, the bridge M–S distance for the M = Mo and W clusters is virtually constant at 2.56–2.57 Å, some 0.08–0.09 Å longer than in Re cluster **8**. This difference is consistent with the six-coordinate Shannon radii difference 0.06–0.07 Å between Mo(III–V) and Re(IV–VI). (v) The shorter mean terminal Fe–SR distance in **8** vs those in **12–14**, by ca. 0.04 Å, is consistent with somewhat more Fe(III) character in the former. Overall, one is impressed more by the dimensional similarities or identities among the 51 and 52 e clusters in Table VII than by the differences. Clearly, all these clusters are electronically delocalized, a property additionally demonstrated by Mössbauer spectroscopy.[11,12,14,26] Mössbauer results for the Re clusters substantiate the Fe(II) bridge structure in **8** and **9**, the subcluster isoelectronic relationship between **7** and **9**, and the somewhat larger Fe(III) character in **8** compared to **12–14**.[26]

Solution Properties. (a) ^1H NMR Spectra. As in past work,[12-14] these isotropically shifted spectra are extremely useful in the identification and assessment of purity of clusters. This is particularly true in the case of the assembly system of Figure 2, where some five cluster species have been detected. At ambient temperature, clusters are strongly paramagnetic with μ_{eff} = 6.5 μ_B (**7**), 8.5 μ_B (**8**), and 9.0 μ_B (**9**) in acetonitrile solutions. The magnetism of these clusters will be discussed elsewhere;[26] here the significant property is the large paramagnetically induced contributions to the chemical shifts, which can lead to exceptional spectral resolution. The spectra of clusters **7–9** are shown in Figures 5 and 6. In general, chemical shifts are somewhat larger and line widths narrower than those of analogous Mo and W clusters, whose previously analyzed spectra[12] provide a basis for signal assignments of the Re clusters.

The most conspicuous feature of the spectrum of cluster **7** (Figure 5) is the appearance of two equally intense signals centered at 62 ppm and separated by 1.4 ppm. This splitting is retained over the interval 240–330 K, being 2.5 ppm at the lowest temperature. These signals can only be assigned to the diastereotopic terminal Fe–SCH_2 protons, a matter confirmed by the presence of a cross peak between the two in a 2-D COSY experiment. Methyl signals of terminal and bridging thiolates are assignable from relative intensities, leaving the sharp singlets at 17.8 ppm as the resonance of the methylene protons of the bridging thiolates.

In cluster **8**, both the terminal Fe–SCH_2 and bridging Re–(SCH_2)–Fe protons are diastereotopic, but their inequivalence is not resolved in the ambient-temperature spectrum (Figure 6). No splitting is observed for the former group in the 253–332 K range. The methyl resonance of the bridging thiolates, connecting two paramagnetic sites, is assigned to the broadened signal at −24.3 ppm; the sharp signal at 12.8 ppm is attributed to the methyl groups of terminal thiolates. The bridging thiolate methylene signals are observed at 253 K as a widely split pair at 169.1 and 46.9 ppm (not shown), which are at or near the slow-exchange limit. As the temperature is raised, these signals broaden and move together, such that at about 290 K they are no longer observable. At higher temperatures, a singlet emerges and occurs at 84 ppm at 332 K. An entirely analogous dynamic behavior has been observed with $[Mo_2Fe_7S_8(SCH_2Ph)_{12}]^{4-}$; possible interpretations of this behavior are given in detail elsewhere.[12] Note that the bridge methylene protons are necessarily anisochronous in the absence of any process that interconverts configurations at the chiral sulfur center. The most likely dynamic process is inversion at sulfur, which equilibrates the methylene protons. The enormous diastereotopic splitting at 253 K (122 ppm) presumably reflects a marked dipolar contribution to the chemical shifts.

Assignment of the spectrum of cluster **9** (Figure 6) follows from that of **8**. At ambient temperature the Fe–SCH_2 resonance is a

(24) Christou, G.; Garner, C. D.; Mabbs, F. E.; King, T. J. *J. Chem. Soc., Chem. Commun.* **1978**, 740.
(25) Shannon, R. D. *Acta Crystallogr.* **1976**, *A32*, 751.
(26) Ciurli, S.; Papaefthymiou, G. C.; Holm, R. H. Results to be published.

Table VII. Comparison of Selected Mean[a] Interatomic Distances (Å) for Double-Cubane Clusters

cluster	M···Fe	Fe···Fe	M–S	Fe–SR[b]	Fe–S	Fe–(μ_2-SR)	ref
$[Mo_2Fe_7S_8(SCH_2Ph)_{12}]^{3-}$	2.73 (1)	2.71 (2)	2.357 (7)	2.256 (4)	2.27 (1)	2.309 (9)	23
$[Mo_2Fe_7S_8(SCH_2Ph)_{12}]^{4-}$	2.73 (1)	2.696 (3)	2.356 (9)	2.252 (3)	2.27 (1)	2.53 (4)	23
$[W_2Fe_7S_8(SCH_2Ph)_{12}]^{4-}$	2.73 (2)	2.695 (2)	2.35 (1)	2.252 (3)	2.272 (7)	2.52 (4)	23
$[Re_2Fe_7S_8(SEt)_{12}]^{2-}$	2.70 (2)	2.70 (1)	2.331 (7)	2.206 (5)	2.26 (2)	2.51 (4)	*c*
$[Re_2Fe_7S_8(SEt)_{12}]^{4-}$	2.76 (2)	2.71 (2)	2.35 (2)	2.24 (2)	2.27 (3)	2.53 (2)	*c*
$[Mo_2Fe_6S_8(SEt)_9]^{3-}$	2.723 (2)	2.687 (3)	2.567 (4)	2.232 (5)	2.26 (1)		11
$[Mo_2Fe_6S_8(SPh)_9]^{5-}$	2.76 (2)	2.70 (2)	2.62 (2)	2.30 (1)	2.28 (2)		14
$[Re_2Fe_6S_8(SEt)_9]^{3-}$	2.739 (1)	2.715 (1)	2.348 (2)	2.232 (3)	2.27 (2)		*c*

[a] The standard deviation of the mean was estimated from $\sigma \cong s = [(|\sum x_i^2 - n\bar{x}^2|)/(n-1)]^{1/2}$ unless the distances are correlated by symmetry. [b] Terminal thiolate. [c] This work.

Table VIII. Comparison of Redox Potentials[a] for Double-Cubane Clusters

cluster	bridge $Fe^{III,II}$	subclusters 52/51 e	subclusters 53/52 e	log K_{com}	ref
$[Mo_2Fe_6S_8(SEt)_9]^{3-}$		−1.28, −1.47	*b*	3.22	*d*
$[Re_2Fe_6S_8(SEt)_9]^{3-}$		−0.27, −0.47	−1.38, −1.62	3.39, 4.07	*d*
$[Mo_2Fe_7S_8(SEt)_{12}]^{3-}$	−0.89	−1.63[c]	*b*		12
$[W_2Fe_7S_8(SEt)_{12}]^{4-}$	−0.76	−1.70,[c] −1.80[c]	*b*		12
$[Re_2Fe_7S_8(SEt)_{12}]^{2-}$	−0.10	−0.58, −0.72	*b*	2.37	10, *d*

[a] Potentials ($E_{1/2}$) reported in V vs SCE in acetonitrile solutions at 297 K. [b] Not observed. [c] E_{pc} values; reductions not resolved for Mo cluster. [d] This work.

singlet, but at about 255 K it splits into a doublet, which persists at lower temperatures. The splitting between the diastereotopic proton signals is 5.4 ppm at 244 K. The behavior of the bridging thiolate methylene signals is very similar to that of **8**. At 244 K, these appear at 152.5 and 48.4 ppm. At higher temperatures they broaden and coalesce. A single peak at 81 ppm is observed at 318 K.

The ^1H NMR spectra of clusters **7–9** satisfactorily demonstrate retention of the bridged double-cubane structures in solution.

(b) Electron-Transfer Reactions. Cyclic voltammetric and differential pulse polarographic results for **7** are presented in Figure 7; the analogous voltammograms for **8** and **9**, recorded under identical experimental conditions, have been reported earlier.[10] Redox potentials are listed in Table VIII, where they are compared with those of the analogous Mo and W clusters. The reactions are not electrochemically reversible, but are chemically reversible in those cases where it was possible to establish that $i_{pc}/i_{pa} \approx 1$.

Cluster **7** exhibits the five-member electron-transfer series (6) with overall charge z = 1− to 5−. Clusters with z = 1−

$$\mathbf{7}: \quad [1-] \overset{E_1}{\rightleftharpoons} [2-] \overset{E_2}{\rightleftharpoons} [3-] \overset{E_3}{\rightleftharpoons} [4-] \overset{E_4}{\rightleftharpoons} [5-] \qquad (6)$$

$$[Re_2Fe_6S_8(SEt)_9]^{-} + [Re_2Fe_6S_8(SEt)_9]^{3-} \overset{K_{com}}{\rightleftharpoons} 2[Re_2Fe_6S_8(SEt)_9]^{2-} \qquad (7)$$

$$[Re_2Fe_6S_8(SEt)_9]^{3-} + [Re_2Fe_6S_8(SEt)_9]^{5-} \overset{K_{com}}{\rightleftharpoons} 2[Re_2Fe_6S_8(SEt)_9]^{4-} \qquad (8)$$

(2[$ReFe_3S_4$]$^{4+}$), 3− (2[$ReFe_3S_4$]$^{3+}$), and 5− (2[$ReFe_3S_4$]$^{2+}$) contain the indicated cores. The redox potentials occur in pairs separated by 190–200 mV. Clusters of intermediate charge can be generated by the comproportion reactions (7) and (8) in acetonitrile solution, for which log $K_{com} = (E_n - E_{n+1})/0.059 = 3.39$ (n = 1) and 4.07 (n = 3). With attainment of the 52 e level in **7**, the subclusters become much more difficult to reduce, and E_3 and E_4 are shifted to more negative values by 1.0 V compared to E_1 and E_2. Cluster **10** and $[W_2Fe_6S_8(SEt)_9]^{3-}$ are not reversibly oxidized but are reduced at similar potentials to form the electron-transfer series z = [3−] ⇌ [4−] ⇌ [5−]. For the comproportionation reaction [3−] + [5−] ⇌ 2[4−], log K_{com} = 3.56 Potentials for the reductions of the 51 e cores in the clusters $[Mo_2Fe_6S_8(SEt)_9]^{3-,4-}$ are ca. 1 V more negative than those for $[Re_2Fe_6(SEt)_9]^{-,2-}$, primarily because of the larger negative charges of the Mo clusters.

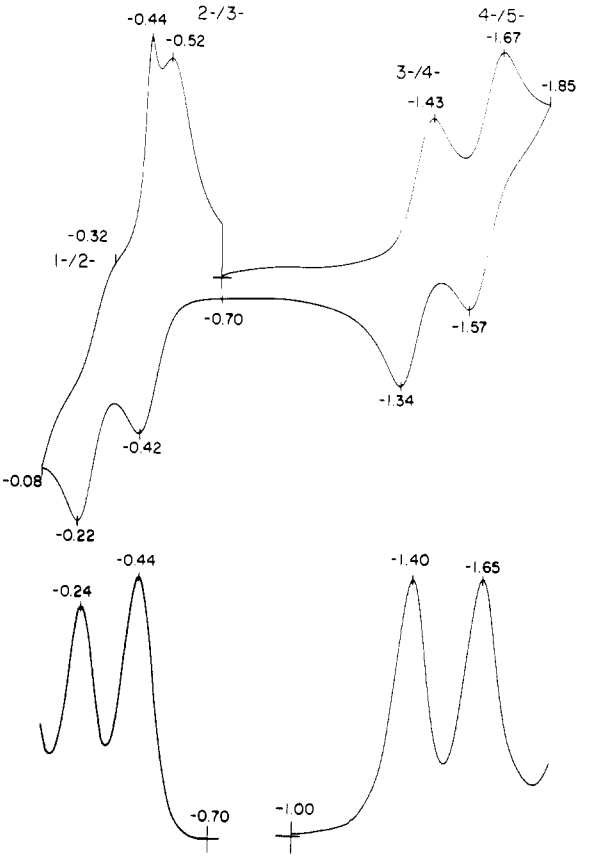

Figure 7. Redox reactions of the cluster $[Re_2Fe_6S_8(SEt)_9]^{3-}$ (**7**) in acetonitrile solution: top, cyclic voltammogram; bottom, differential pulse polarogram. Peak potentials are indicated. The sharp peak at −0.44 V in the cyclic voltammogram is apparently due to an adsorbed species. The voltammograms of **8**/**9** are given elsewhere.[10]

Cluster **8** displays the four-member electron-transfer series (9). By analogy to **12–14**,[12] step E_1 is assigned to reduction of the

$$\mathbf{8}: \quad z = [1-] \overset{E_1}{\rightleftharpoons} [2-] \overset{E_2}{\rightleftharpoons} [3-] \overset{E_3}{\rightleftharpoons} [4-] \qquad (9)$$

bridge Fe atom; steps E_2 and E_3 are subcluster reductions to the [$ReFe_3S_4$]$^{3+}$ (52 e) level. The much larger separation of subcluster potentials (140 mV) compared to that of the Mo and W clusters (where it is 100 mV or less[12]) is presumably caused by the larger incremental increase in cluster negative charge upon reduction. For the comproportion reaction (10), log K_{com} = 2.37 and the mole

$$[Re_2Fe_7S_8(SEt)_{12}]^{2-} + [Re_2Fe_7S_8(SEt)_{12}]^{4-} \overset{K_{com}}{\rightleftharpoons} 2[Re_2Fe_7S_8(SEt)_{12}]^{3-} \qquad (10)$$

fraction of clusters **8** and **9** is 0.884. Lastly, the first member of series 9 is produced at a potential sufficiently close to that for an irreversible, multielectron process (about 0 V) that it is unlikely this Fe(III)-bridged cluster can be prepared. The Mo and W clusters **12–14** also undergo a similar oxidative process, but their $Fe^{III,II}$ potentials occur at much more negative potentials (Table

VIII). Consequently, both the Fe(III)- and Fe(II)-bridged forms of these double cubanes are synthetically accessible.[12]

Substitution Reactions. The reactions of clusters **7–9** with electrophilic reagents have been carried out to explore the possibility of terminal and/or bridge thiolate substitution, in light of the occurrence of similar reactions with the corresponding Mo and W clusters.[28] Thus the reactions of **7–9** with 1–3 equiv of pivaloyl chloride in acetonitrile solution at room temperature afford cluster disruption in all cases, as evidenced by a drastic decrease in intensity of cluster-bound thiolate resonances. Addition of 6 equiv of pivaloyl chloride results in the separation of black insoluble solids. This behavior contrasts with the Mo and W analogue clusters,[27] which undergo stepwise substitution with acetyl chloride to give as final products $[M_2Fe_6S_8(SR)_3Cl_6]^{3-}$ and $[M_2Fe_7S_8(SR)_6Cl_6]^{3-}$. In these cases, bridge ligands cannot be substituted with retention of core structure.

Reactions with benzenethiol in acetonitrile solutions at room temperature are well-behaved and parallel those of analogous Mo and W clusters. Thus, treatment of **7** with 6 equiv of benzenethiol affords reaction 11, in which all terminal ligands have been

$$[Re_2Fe_6S_8(SEt)_9]^{3-} + 6PhSH \rightarrow [Re_2Fe_6S_8(SEt)_3(SPh)_6]^{3-} + 6EtSH \quad (11)$$

substituted. The product cluster has signals at −5.08 (*p*-H), −3.61 (br, CH_3), 15.7 (*m*-H), and 19.5 ppm (br, CH_2) (compare with Figure 5); the *o*-H signal, which will be substantially broader than the others, was not located. Similarly, reaction 12 results when

$$[Re_2Fe_7S_8(SEt)_{12}]^{2-} + 6PhSH \rightarrow [Re_2Fe_7S_8(SEt)_6(SPh)_6]^{2-} + 6EtSH \quad (12)$$

6 equiv of benzenethiol is added to cluster **8**. Terminal ligand resonances are eliminated, and new signals appear at −30.1 (br, CH_3), −5.53 (*p*-H), and 15.2 ppm (*m*-H) (compare with Figure 6). The *o*-H and bridge CH_2 signals were not located in the room-temperature spectrum. Attempts to substitute bridge thiolates in **7** and **8** by adding 9 and 12 equiv of benzenethiol, respectively, resulted in no further reaction in both cases and decomposition of the cluster formed in reaction 12 after 24 h. Cluster **9** with 6 equiv of benzenethiol gave ^1H NMR evidence of terminal ligand substitution (signals at −29 (br), −5.65, and 16.7 ppm), but this species decomposed upon the addition of 3 equiv or more of the thiol.

Summary and Conclusions. The following are the principal findings and conclusions of this work.

(1) The clusters $[Re_2Fe_6S_8(SEt)_9]^{3-}$ (**7**) and $[Re_2Fe_7S_8(SEt)_{12}]^{2-,4-}$ (**8**, **9**) can be prepared as pure solids in high yields in assembly systems containing $(Et_4N)[ReS_4]$, $FeCl_2$, and NaSEt in protic solvents. Clusters **8** and **9** can be interconverted by redox reactions using $(Cp_2Fe)[BF_4]$ and NaSEt, whereas **7** is the product of thermal decomposition of **8** and **9**.

(2) The clusters contain pairs of novel cubane-type $[ReFe_3S_4]$ cores bridged through the Re atom by three thiolates (**7**) or by a trigonally distorted $Fe(SEt)_6$ unit (**8**, **9**). These species are congruent in structure with the previously prepared clusters $[M_2Fe_6S_8(SR)_9]^{3-}$ and $[M_2Fe_7S_8(SR)_{12}]^{3-,4-}$ (M = Mo, W).

(3) Structural, magnetic, and spectroscopic[26] evidence establishes the presence of Fe(II) in the bridge units of **8** and **9**, thereby defining the subcluster core oxidation states $2[ReFe_3S_4]^{4+}$ and $2[ReFe_3S_4]^{3+}$, respectively. The subclusters of **7** and **9** are isoelectronic. Potential differences vs structurally analogous, isoelectronic Mo and W clusters are controlled mainly by charge differences, the Re clusters being 2 charge units more positive.

(4) Cluster **7** supports a five-member electron-transfer series $[Re_2Fe_6S_8(SEt)_9]^z$ (z = 1− to 5−), while clusters **7** and **8** are part of the four-member series $[Re_2Fe_7S_8(SEt)_{12}]^z$ (z = 1− to 4−). In these series, subcluster core oxidation levels vary from $[ReFe_3S_4]^{4+}$ (51 e) to $[ReFe_3S_4]^{2+}$ (53 e).

(5) Clusters **7** and **8** undergo stoichiometric terminal ligand substitution with 6 equiv of benzenethiol to afford $[Re_2Fe_6S_8(SEt)_3(SPh)_6]^{3-}$ and $[Re_2Fe_7S_8(SEt)_6(SPh)_6]^{2-}$, respectively. Attempts to substitute bridge thiolates by use of larger quantities of thiol resulted in no reaction or cluster decomposition. Reactions with <6 equiv of pivaloyl chloride resulted in cluster decomposition. Analogous Mo and W clusters undergo stoichiometric terminal ligand substitution with both reagents and are stable in the presence of excess thiol. These and other observations indicate that the Re clusters are less robust than their Mo and W counterparts, with the general stability order **7** > **8** > **9**.

(6) These new compounds extend the set of heteronuclear MFe_3S_4 cubane-type clusters, which is now constituted of molecules with M = V, Mo, W, and Re. These clusters defined a stability plateau associated with cores containing 51–53 e, with a special stability associated with the 51 e isoelectronic set $[VFe_3S_4]^{2+} = [MoFe_3S_4]^{3+} = [WFe_3S_4]^{3+} = [ReFe_3S_4]^{4+}$.

Finally, as one indication of attractive reactivity properties, cluster **8** and **9** has been cleaved with 1,2-bis(dimethylphosphino)ethane to afford the *single-cubane* cluster **15**, shown in Figure 2. The preparation and structural, electronic, and reactivity properties of **15**, as well as oxidized and reduced forms of this cluster, will be the objects of future reports. Further studies on the reactivity at the Re atom of this new single cubane are also in progress, as well as investigations of alternative ways of bridge cleavage in **8** and **9**, to afford more reactive Re sites.

Acknowledgment. This research was supported by NIH Grant GM 28856. X-ray diffraction equipment was obtained through NIH Grant 1 S10 RR-02247. The authors thank Dr. M. J. Carney for experimental assistance and useful discussions.

Supplementary Material Available: Tables of anisotropic and isotropic thermal parameters, bond distances and angles, and calculated hydrogen atom positions (22 pages); listings of calculated and observed structure factors (91 pages). Ordering information is given on any current masthead page.

(27) Christou, G.; Garner, C. D.; Miller, R. M.; Johnson, C. E.; Rush, J. D. *J. Chem. Soc., Dalton Trans.* **1980**, 2363.
(28) Palermo, R. E.; Power, P. P.; Holm, R. H. *Inorg. Chem.* **1982**, *21*, 173.